Journal of Hazardous Materials 110 (2004) 39–51

Journal of Hazardous Materials

www.elsevier.com/locate/jhazmat

# Recovery of dodecane, octane and toluene spills in sandpacks using ethanol

A.M. Palomino [a,1], D.G. Grubb [b,*]

[a] School of Civil and Environmental Engineering, Geosystems Group, Georgia Institute of Technology, Atlanta, GA 30332-0355, USA
[b] Apex Environmental Inc., 269 Great Valley Parkway, Malvern, PA 19355, USA

Available online 27 April 2004

**Abstract**

This paper is an extension of the work of Grubb et al. [Two-dimensional ethanol floods of toluene in homogeneous, unconfined aquifer media, in: J.C. Evans (Ed.), In-Situ Remediation of the Geo-environment, GSP No. 71, ASCE, NY, 1997, p. 255; Mobilization of toluene in layered, unconfined aquifer media during ethanol flooding, in: P.S.S. Pinto (Ed.), Environmental Geotechnics: Proceedings of the Third International Congress on Environmental Geotechnics Lisboa, Portugal. Balkema Rotterdam Brookfield, 7–11 September 1998] on the recovery of lighter-than-water non aqueous phase liquids (LNAPLs) from sandpacks. Dodecane, toluene and octane (500 mL each) were used to simulate fresh and weathered petroleum spills. The ethanol flooding experiments evaluated the feasibility of recovering the LNAPLs from unconfined uniform sandpacks in a quasi two-dimensional apparatus. A combined pure ethanol and 50/50 (vol.%) ethanol–water blend flooding strategy successfully mobilized and recovered the simulated large-volume LNAPL spills (10× greater than previous studies). At flow rates <7 m per day, the toluene and octane recoveries were approximately 84.9 and 88.1%, respectively, which are considered impressive as no optimization was even attempted.


*Keywords:* LNAPLs; Alcohol flooding; Remediation; Recovery; Petroleum hydrocarbons

## 1. Introduction

Significant problems exist using conventional remediation technologies at sites such as oil refineries which are heavily contaminated with lighter-than-water non-aqueous phase liquids (LNAPLs, e.g., petroleum hydrocarbons). Residual oil saturation and the trapping of LNAPLs above and below the water table by capillary forces make LNAPLs extremely difficult to mobilize under conventional hydraulic gradients for purposes of well-head recovery. This includes well-skimming technologies which cannot recover the LNAPLs trapped at residual saturation. The limited solubility of LNAPLs and the large quantities involved make the cleanup very expensive. Additionally, long times are required, including even vadose zone technologies and biological methods. A consequence of these challenges coupled with the risk-based site specific remediation goals (focusing only on the petroleum components that are suspected carcinogens such as benzene, toluene, etc.), emphasis has shifted to managed risk, natural attenuation, and other strategies that consider actual NAPL recovery as a last resort.

Thus, even the enterprise of using enhanced flooding techniques to accelerate NAPL recovery is more academic than commercial, unless of course we are speaking of enhanced oil recovery which is a mainstay of the petroleum industry. The issue is really one of gestalt, and many environmental practitioners appear to have lost sight of the fact that large LNAPL spills (crude or refined) are natural resources with substantial commercial value, or they lack the entrepreneurial skills to harness this unique opportunity. While environmental agencies may posture toward and/or regulate the treatment and disposal of these spilled materials, this practice seems wholly inconsistent with many resource stewardship and recycling initiatives these same agencies also promote.

For example, consider a sand aquifer with a porosity of 30% that is highly contaminated (60% saturated) with high octane gasoline with a retail value of US$ 1.50 per gallon (current US price; low by world standards). One cubic meter of this soil represents a retail value of approximately US$

* Corresponding author. Tel.: +1-610-722-9050; fax: +1-610-722-9010.
*E-mail addresses:* angelica.palomino@ce.gatech.edu (A.M. Palomino), dgrubb@apexenv-pa.com (D.G. Grubb).
[1] Tel.: +1-404-385-0063; fax: +1-404-894-2281.

0304-3894/$ – see front matter © 2004 Elsevier B.V. All rights reserved.
doi:10.1016/j.jhazmat.2004.02.035

71 versus a disposal cost of US$ 106, assuming a soil unit weight of 120 lb/ft$^3$ (18.9 kN/m$^3$) and an average landfill disposal cost of US$ 50 t$^{-1}$. This amounts to a net revenue swing of US$ 177 m$^{-3}$ of soil, which itself is an impressive number, especially considering that thousands of cubic meters of soil are often contaminated below refineries.

Both remediation and risk-based approaches emphasize minimizing the environmental liability (disposal cost) associated with petroleum spills, but no site management approach currently addresses resource recovery, recycling and recouping a portion of the investment already made in the spilled petroleum products, which speaks to the retail value (US$ 71 m$^{-3}$). In short, all vadose zone treatment technologies like air sparging, air stripping, and bioattenuation completely ignore the commercial value of the LNAPLs to offset cleanup costs. This seems financially unsound from a business perspective when other options exist.

Two in situ technologies that can take advantage of the commercial value of the spilled LNAPLs are steam flooding and alcohol flooding, because a substantial portion of the fluids recovered from the subsurface can be directly used as feedstocks to the petroleum refining process without pretreatment (surfactant/LNAPL mixtures require chemical separation). For the background information on steam flooding, the reader is referred to the many publications of Professor Kent S. Udell of the Mechanical Engineering Department of the University of California, Berkeley. Grubb et al. [1,2] outlined and researched the conceptual feasibility of using ethanol to enhance the recovery of petroleum compounds from unconfined, partially-saturated, quasi 2-dimensional sandpacks at the laboratory scale. Good overviews and references for alcohol flooding are presented in Grubb et al. [1], Grubb and Sitar [3,4], Falta et al. [5], Rao et al. [6], and Sillan et al. [7].

This paper represents a continuation of the work of Grubb et al. [1,2] that previously examined the phenomena of ethanol-induced solubilization, mobilization, displacement and recovery of toluene from simulated spills (<50 mL) in an experimental apparatus having a sandpack measuring approximately 0.76 m × 0.76 m × 2 cm wide ($1.155 \times 10^{-2}$ m$^3$). While those spills were easily and quickly recovered using a dual flooding strategy involving a primary flood of pure ethanol followed by a secondary flood of an equivolumetric blend of water and ethanol (herein referred to as 50/50 blend), the spill quantity was considered small relative to the quantity of sand and injected fluids, and the experimental scale.

In the three experiments reported here, 500 mL (each) of dodecane, toluene and octane were injected into separate sandpacks to simulate a relatively large spill of LNAPL (with respect to the experimental scale) that was viewed to be more consistent with a real field setting. While the densities are fairly similar, these LNAPLs were selected because of their broad range of aqueous solubilities, and hence, the observed phenomena should be representative of both fresh and weathered petroleum spills from a solubility perspective.

## 2. Materials

Flow experiments were conducted in unconfined uniform sandpacks in a quasi two-dimensional apparatus simulating aquifer conditions during aggressive remediation conditions ($v$ > 1 m per day) (see Fig. 1). A detailed description of the experimental apparatus, materials and procedures is presented in Grubb et al. [1] and will not be repeated here, except where modifications exist. Briefly, Fig. 1 shows a sandpack area having the dimensions stated above that was viewable through a clear glass front. Ottawa 20/30 quartz sand having a measured hydraulic conductivity of 0.18 cm/s was used in the experiments. A manifold controlled fluid injection into the apparatus through inlets at various elevations, labeled I1 through I9. The tensiometers (T1–T14) were not used in this series of experiments. Liquid sampling ports, labeled S1–S29, were used for removing small liquid samples directly from the internal pore space of the sandpack. A #80 wire mesh screen separated the sandpack from an open annular space created to simulate a recovery well located on the right hand side of the apparatus. Individually operated effluent ports (E1–E10) were used to control water table levels and recover mobilized LNAPL products from the simulated recovery well.

The fluids used in the flow experiments and their relevant properties are listed in Table 1. The ethanol, 50/50 ethanol–water mixture, and LNAPLs were dyed with iodine, giving the ethanol and 50/50 blend an orange appearance, whereas the LNAPLs were magenta colored. Table 1 shows that the 50/50 blend is denser and more viscous than the other pure organic liquids (ethanol, octane, dodecane and toluene).

Pore liquid and effluent samples collected throughout the toluene and octane experiments were analyzed using a gas chromatograph (HP GC 6890) fitted with a flame ionization detector (FID) and thermal conductivity detector (TCD). Calibration curves were first prepared using the experimental liquids (ethanol, octane, toluene, water) diluted with a fully miscible carrier liquid (acetone) at 0, 20, 40, 50, 60, 80 and 100 vol.% ratios. The responses at each ratio were then plotted versus the blending ratio, yielding in a linear relationship.

Using a direct injection auto sampler, a volume of 1 mL was sequentially extracted from each 2 mL sample vial for GC-FID and GC-TCD analysis. The FID was equipped with a packed column using 3% OV-1 on Chromosorb W-HP, 100/120 mesh (Alltech) to determine acetone, ethanol, toluene and octane concentrations. For the octane data set, the GC-FID oven temperature was ramped from 90 to 220 °C at a rate of 20 °C/min with a hold time of 20.5 min. For the toluene data set, the GC-FID oven temperature was ramped from 80 to 225 °C at a rate of 10 °C/min with a hold time of 10 min. The packed column for the TCD was fixed with Haysep P (Alltech). The TCD oven temperature was ramped from 140 to 200 °C at 10 °C/min with a hold time of 12 min to determine the water, ethanol and acetone concentrations to complete the mass balance. A lower detection limit of 1 mg/L was established for both detectors.

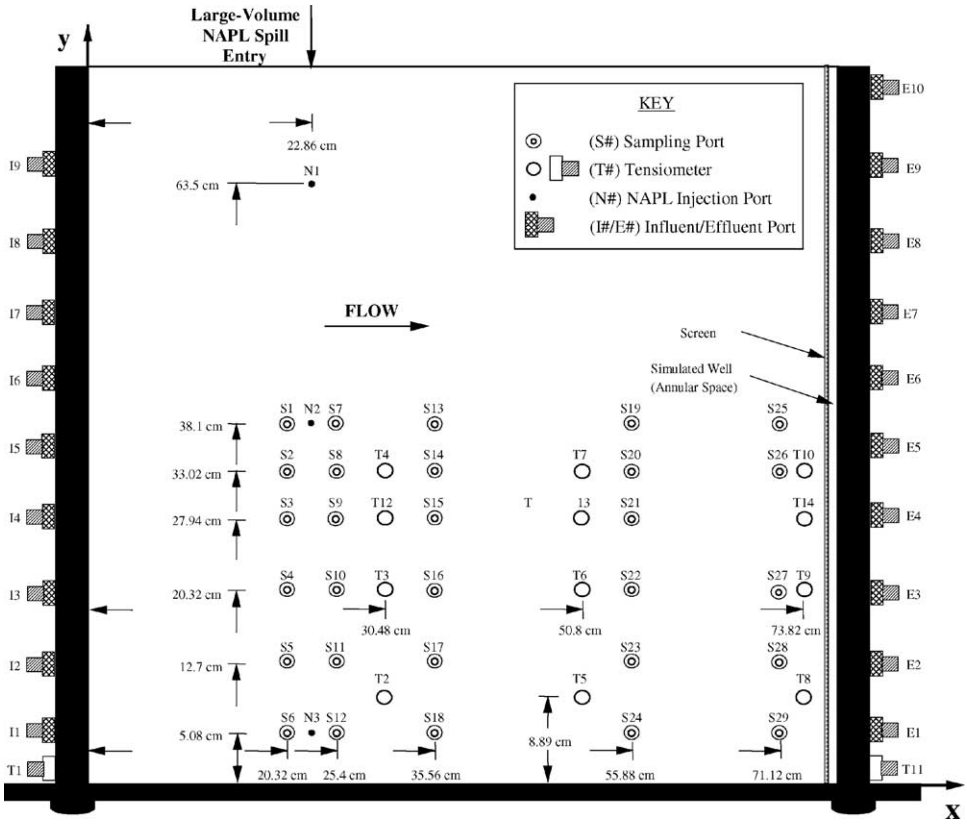


Fig. 1. Schematic of the experimental apparatus showing the layout of the monitoring and sampling devices (after Grubb et al. [1]).

Table 1
Select fluid properties at 25 °C

| Property | Units | Ethanol | Dodecane | Octane | Toluene | Water | Water/ethanol (50/50 vol.%) | PCE | DCM |
|---|---|---|---|---|---|---|---|---|---|
| Aqueous solubility | mg/l | Infinite [9] | 0.0037 [10] | 1.40 [11][a] | 535 [9] | Infinite [1] | Infinite [1] | 150 [14][a] | 13,200 [14][a] |
| Density | g/cm$^3$ | 0.795 [9] | 0.7487 [11] | 0.6986 [11] | 0.8605 [1] | 1.000 [1] | 0.91 [1] | 1.626 [10][a] | 1.325 [14][a] |
| Viscosity | cP | 1.225 [9] | 1.35 [11] | 0.508 [11] | 0.559 [1] | 0.905 [1] | 2.3 [1] | 0.89 [14][a] | 0.43 [14][a] |
| Kinematic viscosity | mm$^2$/s | 1.5 [9] | 1.8 [11] | 0.7 [11] | 0.65 [1] | 0.905 [1] | 2.5 [1] | 0.54 [14][a] | 0.324 [14][a] |
| Vapor pressure | mmHg | | 0.3 [10] | 11 [10] | 20.1 [9] | | | 14 [10][a] | 349 [10][a] |
| Surface tension | dynes/cm | | 25.44 [11] | 21.80 [11] | 29 [13] | 72.75 [12] | | 31 [13] | 26.52 [11] |
| Interfacial tension | dynes/cm | | 52.90 [12][b] | 50.8[12][b] | 36 [13] | | | 44 [13] | |

PCE: perchloroethene; DCM: dichloromethane.
[a] 20 °C.
[b] 20 °C in contact with vapor.

Dodecane data is not reported due to chemical–analytical problems.

## 3. Experimental sequence

The properties of each sandpack were first determined under water flooding conditions. Using a constant water injection rate through I1 and I2, a capillary fringe and water table level were allowed to stabilize. Unlike previous experiments [1,2], 500 mL of LNAPL were released through the top of the apparatus at an elevation of 76 cm, directly above N1. The LNAPL was allowed to gravity drain through a funnel into the sandpack below. The LNAPL migrated vertical downwards and then spread laterally along, and collapsed, the capillary fringe. Product entering the simulated recovery well (far right, Fig. 1) was removed using a product skimmer with an adjustable inlet level that was independently operated through the top of the apparatus and separately from the effluent ports. The skimmer was operated until LNAPL migration into the well ceased, indicating that the LNAPL spill was at residual saturation in both the vadose zone and upper reaches of the water table. This product recovery is later referred to as “drainage” recovery.

A dual flooding strategy as described in Grubb et al. [1] was then employed to mobilize the LNAPL to the recovery well. A primary flood of pure ethanol was initiated in the upper reaches of the water table. This flood was used to

initiate solubilization and mobilization of LNAPL, creating local conditions very rich in ethanol that enabled reduction of interfacial tension (IFT) between the LNAPL and water. After ethanol breakthrough at the recovery well, the water table level could then be manipulated (up/down) to conduct a vertical sweep of the sandpack to recovery LNAPL situated in the vadose zone above the original water table elevation. It was previously observed [1,2] that a secondary flood using the 50/50 blend was strategically very important as this created a viscous wedge of fluid capable of mobilizing stranded LNAPL, and particularly those LNAPLs slightly more dense than pure ethanol. After the 50/50 blend broke through at the recovery well, a follow up (tertiary) water flood was initiated to remove the ethanol from the sandpack.

## 4. Dodecane mobilization experiment

Steady state flow conditions in the apparatus were achieved at 0.380 $cm^3$/s, creating a well elevation of 24 cm and a capillary fringe of 9 cm. The calculated flow velocity and equivalent pore volume (PV) were approximately 6.8 m per day and 1207 $cm^3$, respectively. Five hundred milliliters of dodecane were released into the sandpack well above the water table (above N1). The dodecane migrated downwards, then laterally across the water table, its weight collapsing the capillary fringe. The contaminant reached the recovery well approximately 8 min after the spill. The inlet of the skimming well was set at 25 cm (1 cm above original water table elevation), and approximately 60 mL of dodecane were removed as the spill stabilized. The bulk of the dodecane was situated between elevations 27.5 and 37 cm in the capillary fringe and upper reaches of the phreatic zone. Residual dodecane was trapped in the vadose zone above elevation 37 cm, including the neck of the spill shaft between 15 and 35 cm ($x$-coordinates).

Fig. 2 is a photograph showing the distribution of the dodecane at 60 min, just prior to the ethanol flood. The legend presented in Fig. 2 denotes the presence of LNAPL floating product and water as Zones I and II, respectively. Zone III refers to NAPL emplaced/trapped the vadose zone, and Zone IV denotes the injected ethanol. Residual saturation marks the downward migration and maximum layer thickness of the dodecane (between elevations 40 and 45). Ethanol (primary flood) was introduced at 68 min into inlets I5 and I6, located at elevations 35.5 and 43.2 cm, respectively. The total flow was kept constant by introducing the primary flood at half the original water flow and simultaneously reducing the water injection rate by half. In Fig. 3, downward vertical migration of the LNAPL resulting from IFT reduction can be seen along the leading edge of the sloped ethanol–water interface (dark band), extending downward to elevation 21 cm at the inlet between Zone IV with Zones I and II.

The downward migration of the dodecane temporarily blocked the horizontal flow of the ethanol (left to right) creating a sizeable bank of both dodecane and ethanol near the inlet as shown in Fig. 4, a photograph taken at 82 min. At this time, a thick bank of ethanol (Zone IV) has formed between elevations 17.5 and 45 cm. The creation of this bank is partially attributed to the low solubility and elevated viscosity of dodecane, although a comparison of fluid density suggests that ethanol should under-ride and bypass the dodecane, an effect that becomes manifest in later stages of the flood. In the early stages, however, ethanol had difficulty migrating in, through, and around the dodecane spill (Zones I and III), and fingering of ethanol into the residual contam-

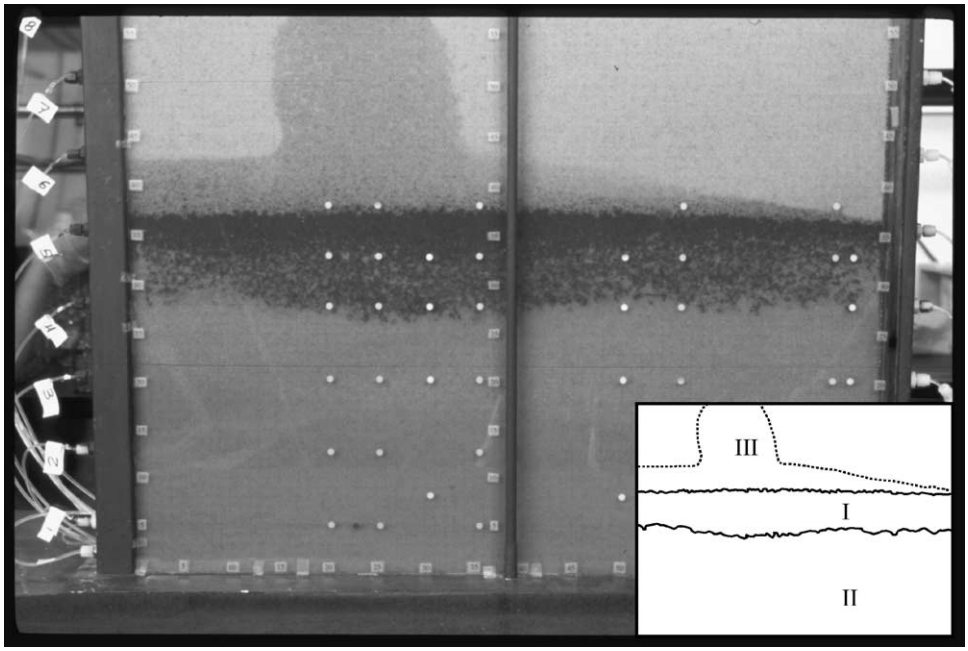


Fig. 2. Dodecane distribution at 60 min, immediately prior to ethanol flood.

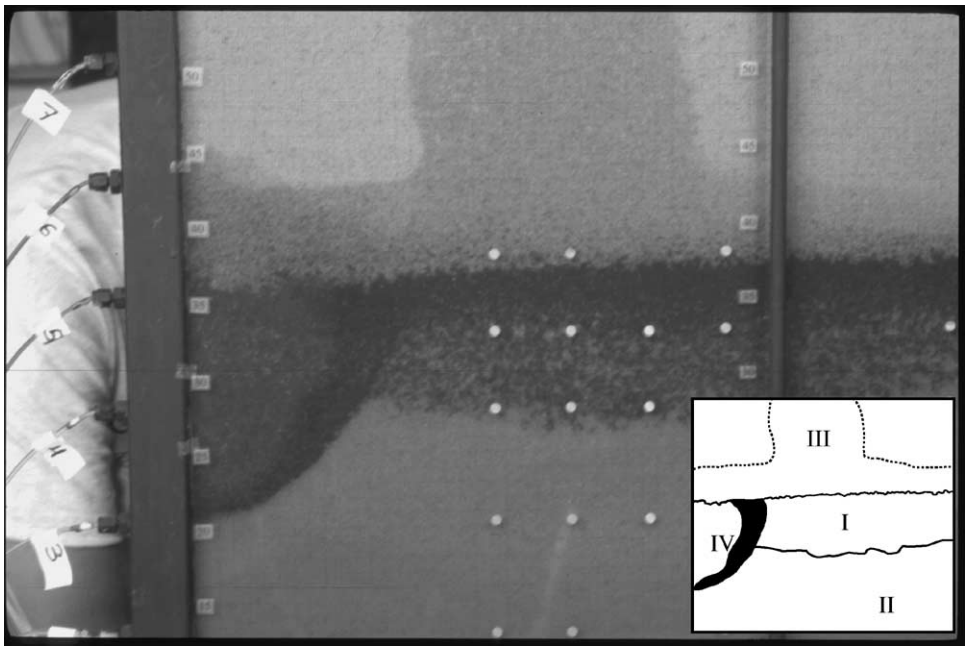


Fig. 3. Primary ethanol flood intersecting dodecane layer at 75 min.

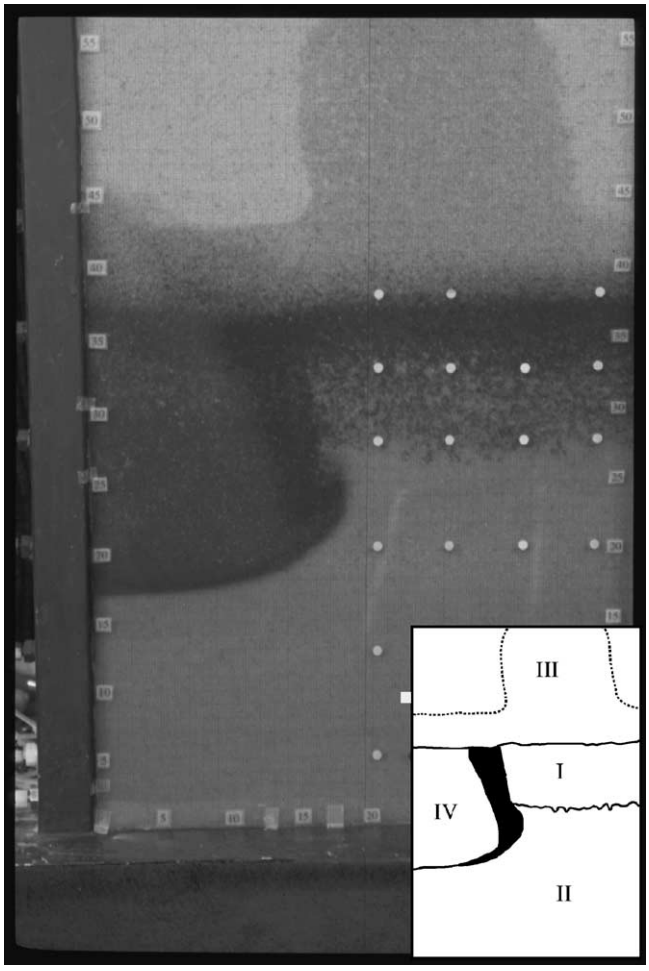


Fig. 4. Primary ethanol flood impeded by banking dodecane, 82 min.

inated zone apparently did not create local concentrations of ethanol sufficiently high enough to break the separate phase due to dodecane's insolubility. However, after sufficient injection of ethanol, the ethanol was finally able to under-ride the less dense dodecane (Zone I), as shown in Fig. 5. By now, a considerable bank of dodecane had formed along the leading edge of the ethanol front, sloping downgradient at approximately 45°.

Ethanol breakthrough occurred at the recovery well at 133 min, and the banking of the dodecane (Zone I) above the ethanol (Zone IV) is clearly evident. Much of the visible product was removed by this time, but a thin layer of LNAPL remained just above the main ethanol front. The LNAPL layer extended horizontally from 20 to 70 cm (*x*-coordinates). An attempt was made to mobilize this dodecane, as well as the residual saturation in the vadose zone, by increasing the groundwater flow and subsequently raising the water table. However, raising the horizontal ethanol–water interface merely stranded a very thin (smear) band of dodecane at the bottom of the ethanol bank between elevations 17.5 and 20 cm across the entire width of the apparatus, as shown in Fig. 6. This effect was also observed for toluene [2], but the key difference here is that dodecane is less dense than ethanol. Accordingly, a key observation is that LNAPLs lighter than the alcohol used for primary flooding can migrate below the alcohol swept zone, making a dual flooding strategy and/or manipulation (lowering) of the water table necessary. Hence, after initial breakthrough, ethanol injection continued for 60 min and a downward vertical sweep was completed by lowering the water table (dewatering of the sandpack). Similarly, and upward sweep can remove residual contaminants from the vadose zone, as shown in Fig. 13.

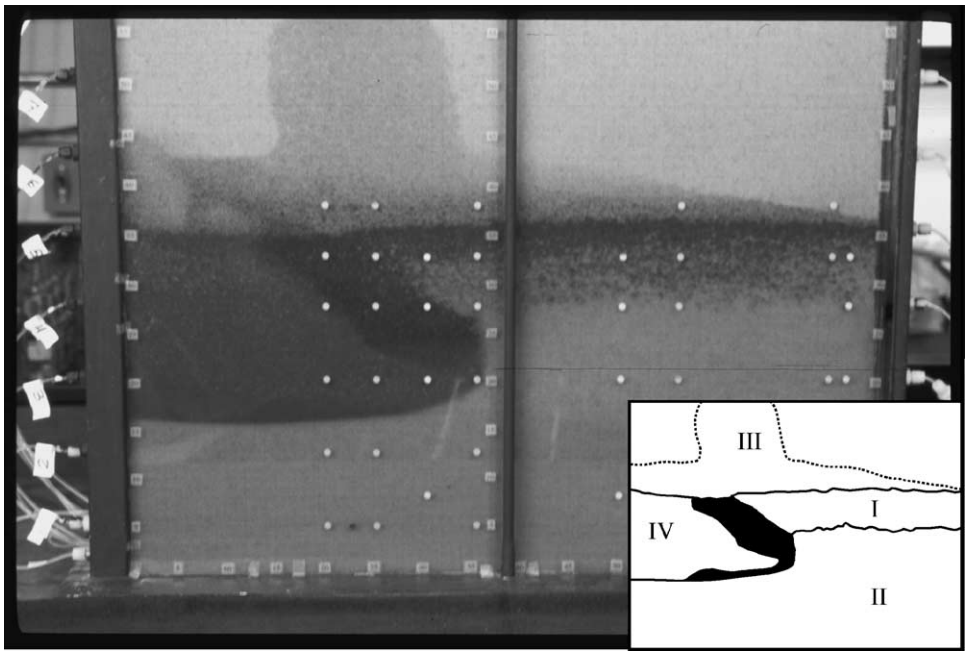


Fig. 5. Lower ethanol layer breaking through dodecane bank, 97 min.

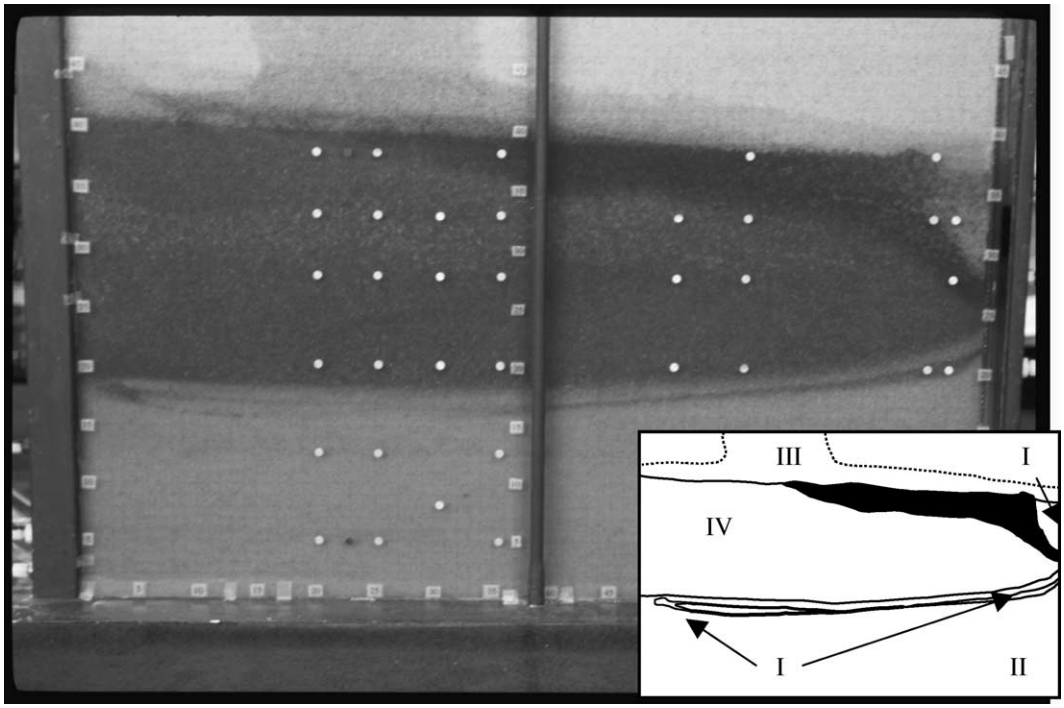


Fig. 6. Line of stranded dodecane just below ethanol layer, between elevation 15 and 25 cm, at 154 min.

At 193 min, the 50/50 ethanol–water blend was injected through inlets I1 and I2 at elevations 5.1 and 12.7 cm, respectively. The secondary flood replaced the groundwater at an injection rate of 0.380 $cm^3$/s. The inlets were specifically selected so the 50/50 blend would migrate both horizontally and upward to intersect the stranded dodecane. The secondary flood continued for 98 min until no visible traces of dodecane remained (291 min). Water flow was then restored to I1 and I2 to flush ethanol from the sandpack.

## 5. Octane mobilization experiment

Steady state flow conditions were achieved in the apparatus at a rate of 0.378 $cm^3$/s creating a well elevation of 24 cm and a 9 cm thick capillary fringe. The calculated flow velocity and equivalent pore volume were approximately 6.8 m per day and 1353 $cm^3$, respectively. Five hundred milliliters of octane were released into the apparatus, initiating the spill well above the water table. Octane migrated downwards,

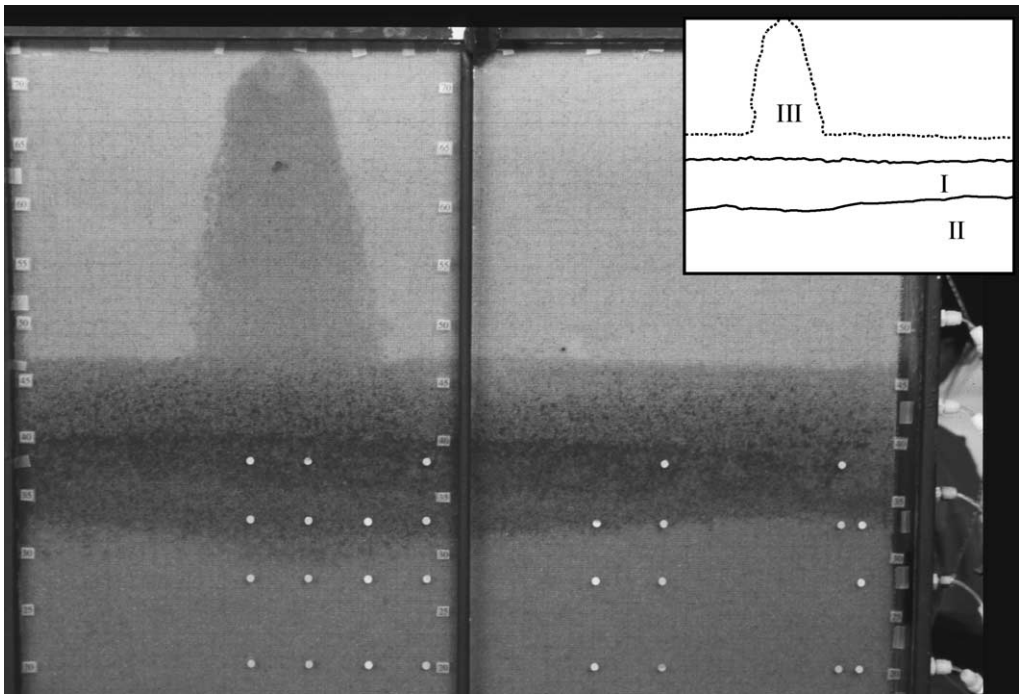


Fig. 7. Octane distribution at 90 min, immediately prior to primary flood.

then laterally, its weight collapsing the capillary fringe. The octane reached the recovery well in approximately 20 min. The inlet of the skimming well was set at 25 cm (1 cm above original water table elevation), and 220 mL of octane were removed as the distribution stabilized after about 90 min.

Small-volume samples (∼2 mL) were extracted from the sampling ports to establish baseline conditions. For example, the concentration of octane prior to ethanol injection was 715,000 mg/L at sample port S1. A note about concentrations: the value of 715,000 mg/L is obviously above that predicted based on the octane fluid density (∼698,000 mg/L), which is also temperature dependent. While analytical accuracy at both ends of the spectrum was good (<1%), the effects of errors are highly magnified in very concentrated organic liquid systems. For pure octane, one percent error on the upper end (purity) becomes 6980 mg/L. Hence, the value of 715,000 mg/L is certainly within 2% and is still considered reliable.

Fig. 7 shows the distribution of octane (Zones I and III) just prior to the ethanol flood. Ethanol was injected into the apparatus through inlets I5 and I6 at 100 min. The ethanol flow was set at half the water flow, and the water flow was also reduced so that the total flow rate remained constant. After the ethanol front encountered the octane, the horizontal flow of ethanol was impeded in much the same way as shown in Figs. 3 and 4, though less dramatic owing to the lower density and viscosity of the octane.

Fig. 8 shows the geometry of the ethanol front (Zone IV) at 147 min, illustrating that octane remained situated above the pure ethanol at all times. In essence, the leading edge of the ethanol formed a wedge-shaped front that separated the mobilized octane layer (dark region above) from the water phase (below). Ethanol broke through at the recovery well at 150 min. The ethanol injection continued for an additional 52 min, until 199 min. During this interval, the underlying water flow rate was increased to conduct an upward vertical sweep of the vadose zone using the bank of ethanol to mobilize octane trapped at residual saturation.

After 199 min, no visible traces of octane were left within the region swept by ethanol. However, a small region of stranded octane was observed near influent port I3. An attempt was made to mobilize this stranded octane by initiating the 50/50 blend through inlets I3 and I4 at 202 min. The 50/50 blend was injected for 68 min, during which time some, but not all, of the stranded octane was mobilized. Following the 50/50 flood, pure water was injected through inlets I1 through I4 to remove the remaining ethanol.

Analyzed pore liquid samples indicated that octane was very mobile during the experiment. For example, initial concentration of octane of 715,000 mg/L at S1 was reduced to a non-detect after passage of the ethanol front. No additional samples were taken at S1 after the 50/50 flood was initiated due to the shift in elevation of the water table. At S3, the passage of the ethanol front was associated with a reduction in octane concentrations from 702,000 to 43.7 mg/L. Octane concentrations at S10 were reduced from 189,000 to 103,000 mg/L just prior to 50/50 flood, which was further reduced to 806 mg/L. The initial octane concentration at S23 was non-detect (<1 mg/L), as the port was located well below the water table and the lowest extremity of the initial octane spill. While the pure ethanol flood did not encounter S23, the subsequent 50/50 blend passed by this port carry-

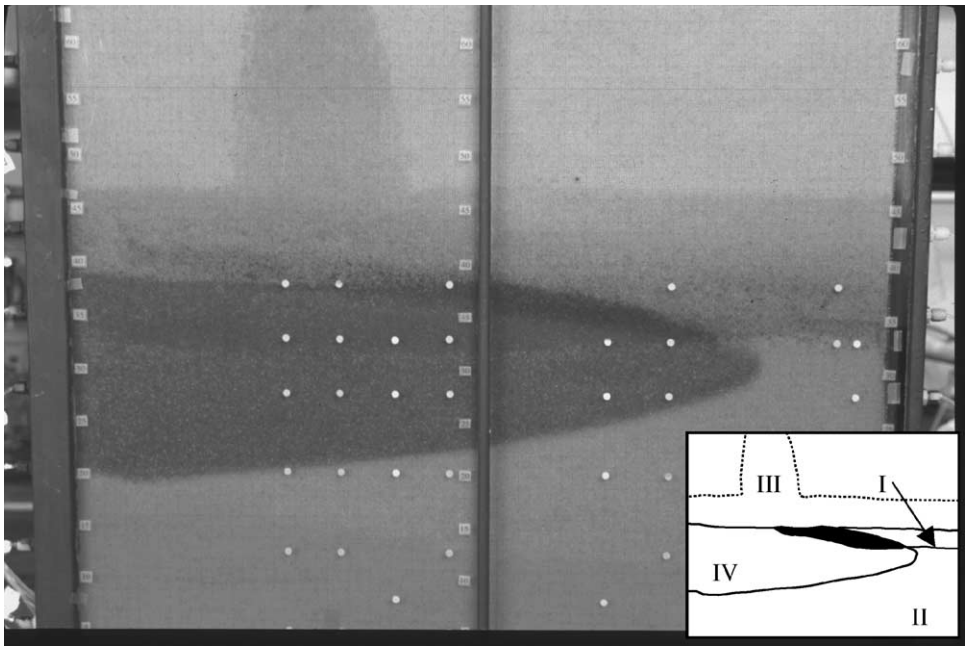


Fig. 8. Wedge-shaped ethanol flood at 147 min separating the less dense octane (top) from the denser water phase (bottom).

ing approximately 137 mg/L of octane which later dropped to non-detect. Octane concentrations at S28 and S17 were similar to those for S23, with zero concentration at S28 and 346 mg/L at S17 prior to the 50/50 flood, increasing to 7980 mg/L (S28) and 19,600 mg/L (S17) during the 50/50 flood. Both returned to non-detects after the 50/50 blend had passed.

Fig. 9 shows the cumulative octane and ethanol recovery as percentages of the totals released. The gravity drainage of the octane accounted for 51.5% recovery (257.5 mL), an elevated value that is partially attributed to octane's low density (versus dodecane, toluene), making it more likely to flow into the well instead of suppressing the capillary fringe. Primary recovery of octane was measured at 27% (135 mL). The subsequent 50/50 blend mobilized an additional 9.2%. The *x*-axis of Fig. 9 shows the quantities of liquids simultaneously and/or sequentially injected including water, ethanol and the 50/50 blend as the experiment evolved. The total volume of ethanol and 50/50 blend injected were 1300 and 900 mL, respectively, over an experiment duration of 267 min.

The total percentage of octane recovered was 88.1%. The pore liquid samples extracted during the flow experiment accounted for an additional 15.8 mL of octane, or 3.2%. It is important to note that the entire vertical height of the apparatus was intentionally not swept by ethanol. Accordingly,

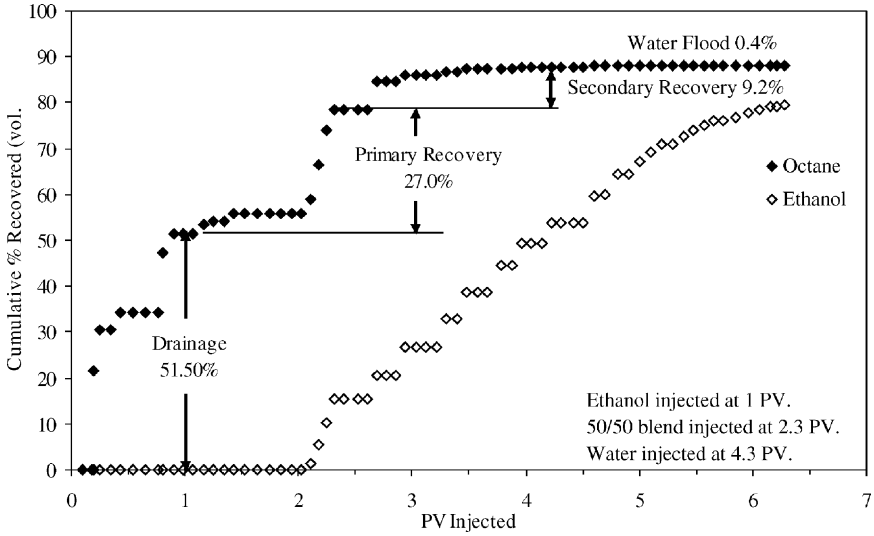


Fig. 9. Cumulative octane and ethanol recoveries as percentages of quantities released.

the missing 8.7% of octane is attributed to residual saturation above the ethanol swept zone (i.e., Zone III), volatilization losses to the vadose zone and from the effluent collection bottles during experimentation, and operator error. Mass losses due to volatility are believed to be the primary factor for the following reasons: octane is very volatile; the vadose zone of the sandpack was larger than the saturated zone; experimentation required the use of (hot) flood lamps for illumination, and the effluent bottles (250 mL) used in experimentation remained open during filling operations to avoid back-pressuring of the experimental apparatus. Lastly, the effluent bottles were located in a vacuum hood for safety reasons. Given these factors, the mass balance is considered to be very good.

## 6. Toluene mobilization experiment

Steady state flow conditions were achieved in the apparatus at a rate of 0.383 $cm^3$/s creating a well elevation of 25 cm and a 9 cm thick capillary fringe. The calculated flow velocity and equivalent pore volume were approximately 6.6 m per day and 1429 $cm^3$, respectively. Five hundred milliliters of toluene were released into the apparatus, initiating the spill well above the water table. Toluene migrated downwards, then laterally, its weight collapsing the capillary fringe, reaching the recovery well in approximately 6 min. The inlet of the skimming well was set at 26 cm (1 cm above original water table elevation), and 120 mL of toluene were removed as the spill stabilized at 41 min.

Fig. 10 is a photograph taken 44 min after the release, just prior to the ethanol flood. The narrow characteristic shaft of downward migrating LNAPL (Zone III) is clearly evident in the top left in the vadose zone, as well as the residual saturation markings showing the maximum thickness of the banked LNAPL between elevations 40 and 45 cm during the early stages of the spill. Much of this LNAPL drained into the well and compressed the capillary fringe. The bulk of the toluene prior to ethanol flooding was located between elevations 25 and 35 cm in the upper reaches of the water table.

Ethanol was introduced into the sandpack through I3 and I4 (elevations 20.3 and 27.9 cm, respectively) to intersect the phreatic surface. As the ethanol propagated through the apparatus and co-mingled with the denser toluene, the sudden IFT reduction allowed the toluene to drain downwards along the sloping ethanol–water interface thereby impeding the horizontal flow of ethanol, as shown in Fig. 11 (Zone IV; dark band). Also, the bank of toluene migrated horizontally ahead of the ethanol, achieving very high concentrations. For example, as the ethanol front passed sampling ports S1, S2, and S3, measured toluene concentrations were on the order of 854,000, 849,000 and 847,000 mg/L, respectively. Similar toluene concentrations were later measured at S8, S9, S15, S20, and S21 during the primary flood.

The continued drainage of toluene down the ethanol–water interface (Zone IV/I) caused a bank of ethanol of increasing thickness to form, and stalled the movement of the lower portion of the ethanol front (i.e., bottom of Zone IV). With time, the upper portion of the front migrated ahead of the stalled bottom portion of the front. This effect is shown clearly in Fig. 12, as the position of the lower portion of the front remained essentially unchanged between Figs. 11 and 12. The decrease in pressure associated with the vertical drainage of the toluene, and the horizontal movement of the upper portion of the ethanol front thinned the bank of

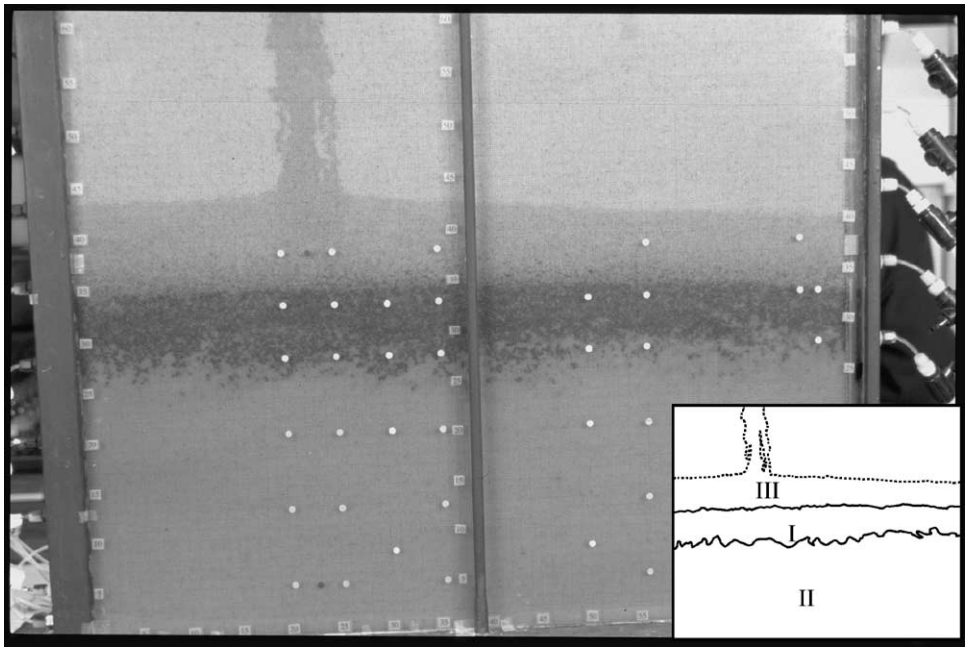


Fig. 10. Toluene distribution at 44 min, immediately prior to ethanol flood.

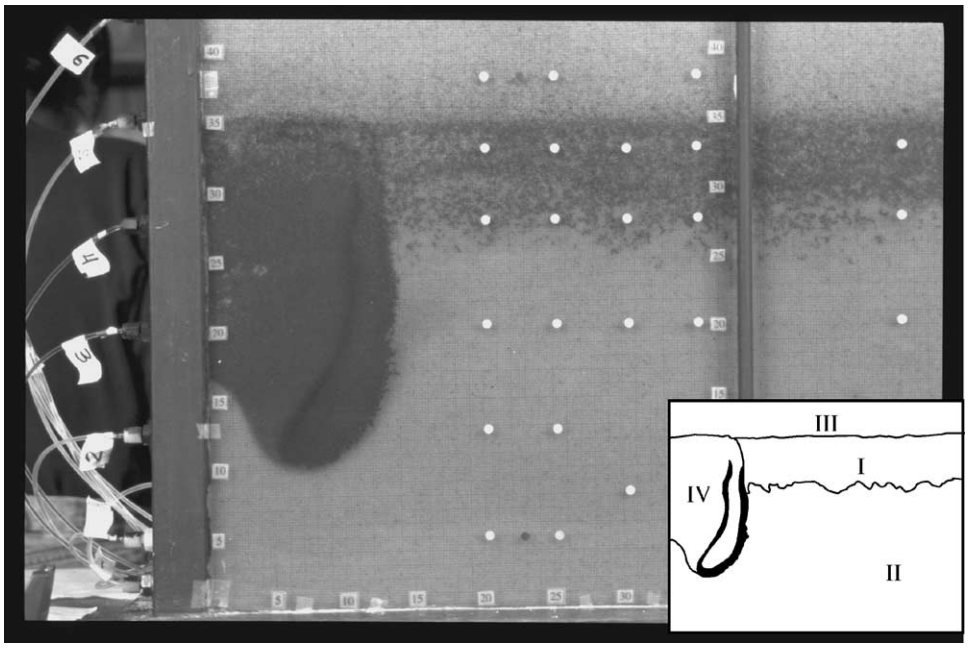


Fig. 11. Horizontal migration of primary ethanol flood impeded by toluene (darkest band) situated along the ethanol–water interface at 99 min.

ethanol, which subsequently rose upwards under buoyancy. This flow sequence stranded the toluene in the lower portion of the sandpack with between (*x*, *y*) centimeter coordinates (5, 10) and (14, 13) measured from the lower left of Fig. 1.

Ethanol broke through at the recovery well at 99 min and flooding was continued for another 50 min. By this time, most of the toluene had been swept from its initial position (between elevations 25 and 40 cm). Some of the mobilized toluene formed a stranded band between elevations 10 and 20 cm across the entire reach of the sandpack, as shown in Fig. 13.

At 149 min, the pure ethanol was replaced with the 50/50 blend to recover the stranded toluene. The 50/50 flood was continued for 68 min, after which time no visible traces of toluene were observed. The flow phenomena associated with the 50/50 blend and the recovery of the stranded toluene were identical to previous toluene recovery experiments [1,2]. The sandpack was then water-flooded to remove the ethanol.

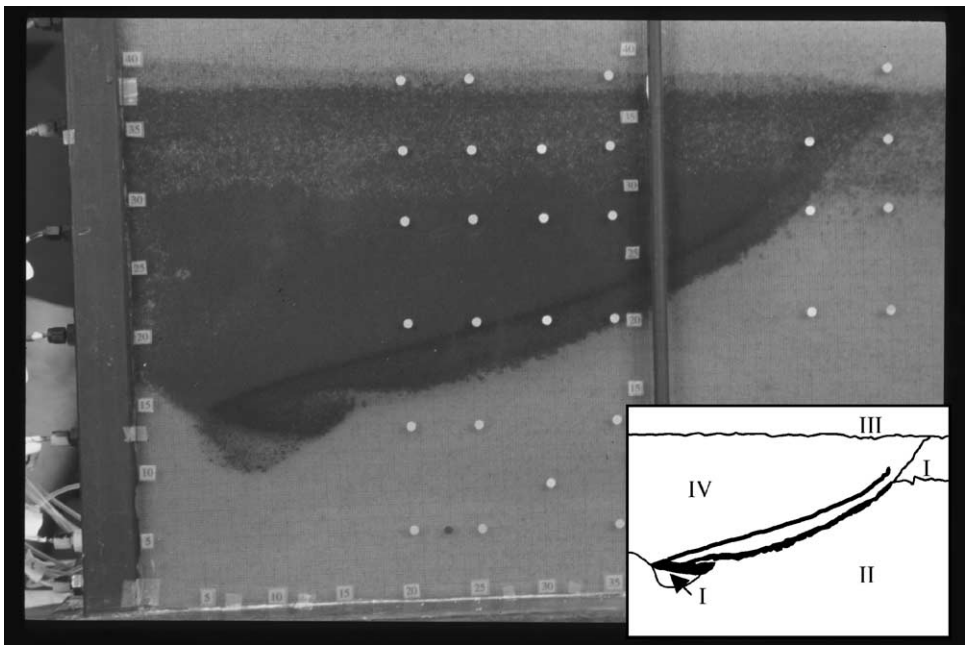


Fig. 12. Top portion of ethanol front advancing beyond the stalled lower portion at 83 min. Stranded toluene ganglia are visible between coordinates (5, 10) and (14, 13).

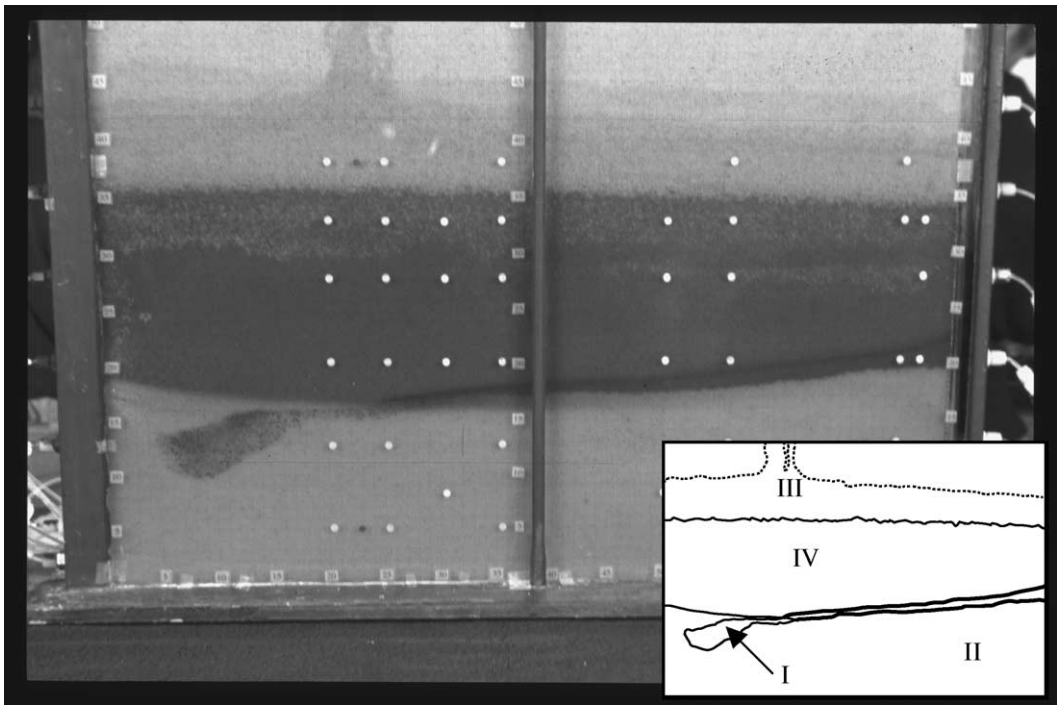


Fig. 13. Stranded toluene ganglia along the bottom of the ethanol–water interface between elevations 10 and 20 cm at 125 min.

After the follow-up waterflood, pore liquid samples were obtained to determine cleanup efficiency. Pore liquid samples could not be obtained at S1, S2, S3, S8, S9, S15, S20, and S21 due to the lowering of the water table below these ports. The toluene concentration at S4 was reduced from 752,000 mg/L during the primary ethanol flood to 264 mg/L at experiment end. Similar results were obtained at S5, S16, S17 and S28. No toluene was detected at S6, S18, S24, and S29.

Fig. 14 presents the cumulative recoveries of toluene and ethanol as percentages of the quantities released. Gravity drainage of toluene amounted to 24% (120 mL) prior to ethanol injection. Primary recovery, i.e., that associated with the pure ethanol was approximately 45.7% (228.5 mL) over 1.8 pore volumes prior to the injection of the 50/50 blend. The injected 50/50 blend mobilized an additional 14.5% (72.5 mL) of toluene over the next 2.4 pore volumes. The total volume of ethanol and the 50/50 blend injected were 1500 and 1600 mL, respectively, prior to termination of the experiment at 217 min. Approximately 0.6% of the toluene was recovered after the follow-up waterflood was initiated.

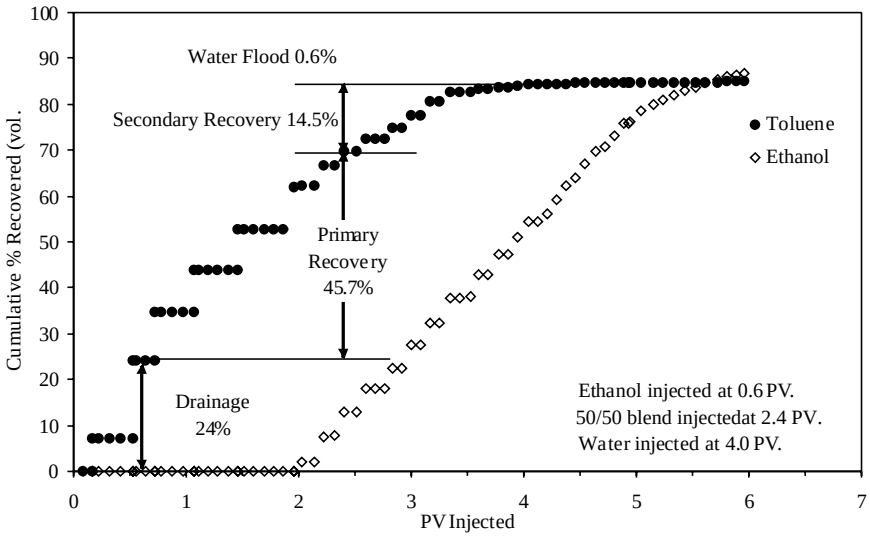


Fig. 14. Cumulative toluene and ethanol recoveries as percentages of quantities released.

Table 2
Flooding conditions for mobilization experiments

| Condition | Units | Dodecane | Octane | Toluene |
|---|---|---|---|---|
| Initial conditions | | | | |
| Well elevation | cm | 24 | 24 | 25 |
| Capillary fringe thickness | cm | 9 | 9 | 9 |
| Spill conditions | | | | |
| Time to NAPL breakthrough | min | 8 | 20 | 6 |
| Time to stabilize | min | 60 | 90 | 41 |
| Drainage recovery | mL | 60 | 220 | 120 |
| Pre-flood conditions | | | | |
| Well elevation | cm | 23 | 25 | 23 |
| Capillary fringe thickness | cm | 5 | 7 | 2 |
| Time ethanol injected | min | 68 | 100 | 44 |
| Time to ethanol breakthrough | min | 133 | 150 | 99 |
| Ethanol injected | mL/PV | 1400/1.16 | 1300/0.96 | 1500/1.05 |
| 50/50 blend injected | mL/PV | 1500/1.24 | 900/0.67 | 1600/1.12 |

PV: pore volumes.

Toluene recovery was estimated at 84.9% (424.5 mL). The volume of toluene associated with the collected pore liquid samples was estimated to be 28.7 mL, or 5.7%. As before, it is important to note that the entire vertical height of the apparatus was intentionally not swept by ethanol. Accordingly, the missing 9.4% of toluene is attributed to the same factors as the octane experimental conditions.

## 7. Discussion

Interesting phenomena was observed related to the shapes of the spills in the vadose zone for similar release conditions, i.e., the necks of the spill columns or shafts (Zone III) shown in Figs. 2 (dodecane), 7 (octane) and 10 (toluene). Schwille [8] expected that the narrowness of the spill penetration (shaft) should be related to the kinematic viscosity ($\nu$) of the released NAPL. That is, increasingly narrow shafts should be correlated with decreasing kinematic viscosities, as the resistance to flow is obviously less, see Table 1 for property data. Schwille observed the opposite of this trend with his infiltration experiments involving percholorethene (PCE) and dicholoromethane (DCM), and attributed the increased lateral spreading of the least kinematically viscous NAPL (DCM) during infiltration to its higher vapor pressure. Comparison of Figs. 2, 7 and 10 and the data presented in Table 1 indicate that our results follow neither of these trends: Toluene has the highest vapor pressure but the narrowest infiltration pattern (Fig. 10) even though it has virtually the same kinematic viscosity as octane. Dodecane, the least soluble and volatile, has the widest spreading infiltration pattern of the three compounds (Fig. 2). It is likely that the infiltration pattern of NAPLs in dry porous media therefore is a complex function of the physical and interfacial properties, including the surface and interfacial tensions, and spreading coefficients. The two sets of experimental data (these and [8]) suggest that compounds with high surface tensions (toluene and PCE) spread less during infiltration in dry soils which may give rise to the narrowness of the infiltration patterns. As reduced lateral spreading allows for NAPL vertical heads that drive flow to be more quickly established during infiltration, these artifacts may also contribute to the narrowness of the infiltration patterns.

Table 2 gives a comparison of the experimental results and shows that octane had the most volume recovered during spill initiation (drainage). NAPL breakthrough at the well during spill initiation and the time for the spill to stabilize was not a strong function of kinematic viscosity, but the results do suggest that low density and viscosity NAPLs have a tendency to accumulate in recovery wells and have the least overall ethanol flooding requirements during remediation. This is not just related to the high drainage recovery of the octane. Comparison of Figs. 2, 7 and 10 indicates that the octane spill sat the highest in the sandpack and that it penetrated the least into the phreatic zone, thus suggesting less volume of soil to be swept by the ethanol. Toluene is associated with the highest compression of capillary fringe due to its density, but accumulates more in the well during spill initiation than dodecane, presumably due to the lower viscosity of dodecane. Despite its higher density, toluene requires less overall ethanol requirements (2.17 PV versus 2.40 PV) than dodecane primarily due to the lower solubility and higher viscosity of dodecane. Despite the physical property differences in the LNAPLs and the attendant migration phenomena, the dual flooding strategy was able to achieve very high recoveries of each compound (visually implied for dodecane) for relatively minor pore volume requirements.

## 8. Concluding remarks

Given the experimental scales involved, three relatively large LNAPLs spills were created in unconfined uniform sandpacks in a quasi two-dimensional apparatus. Dodecane, toluene and octane (500 mL each) were used to simulate fresh and weathered petroleum spills. A combined pure

ethanol and 50/50 (vol.%) ethanol–water blend flooding strategy successfully mobilized and recovered the LNAPL spills in a matter of hours. At flow rates <7 m per day, no visible traces of the dodecane remained, while the octane and toluene recoveries were approximately 88.1 and 84.9%, respectively. These percentages are considered impressive since no optimization was even attempted. As before [1,2], the LNAPLs, ethanol, 50/50 blend and water were strongly stratified according to density in both the sandpack and recovery well. This phenomena enabled gravimetric separation of the liquids as the liquid–liquid interfaces separating a highly concentrated ethanol–LNAPL mixture positioned over essentially clean water were on the order of 1 cm in thickness. These conditions make it very easy and advantageous to recover and recycle the concentrated ethanol–LNAPL mixture as a feedstock to the petroleum refining process. These simple experiments illustrate that large quantities of spilled petroleum products have the potential to be recovered in very short timeframes. If a local refinery exists, the ethanol flooding strategy suggests that the recovery and recycling of the recovered ethanol–LNAPL mixture could be cost effective relative to other site management and restoration strategies that have LNAPL treatment and disposal as primary outcomes.

## Acknowledgements

Drs. Grubb and Palomino performed this work at Georgia Tech under sponsorship of NSF CAREER Award CMS 9703367. Additional support was provided by the School of Civil & Environmental Engineering. The authors are grateful for the assistance of W.E. Diesing III, M. Guimaraes, G. Kolb, D. Landers, Kasemchart Shriwalai, and R. Valencia who assisted with the flooding experiments.

## References

[1] D.G. Grubb, L.E. Empie, G.W. Hudock, R.N. Davies, S.B. Lathrop, Two-dimensional ethanol floods of toluene in homogeneous, unconfined aquifer media, in: J.C. Evens (Ed.), In-Situ Remediation of the Geo-environment, GSP No. 71, ASCE, NY, 1997, pp. 255–270.

[2] D.G. Grubb, L.E. Empie, G.W. Hudock, R.N. Davies, S.B. Lathrop, Mobilization of toluene in layered, unconfined aquifer media during ethanol flooding, in: P.S.S. Pinto (Ed.), Environmental Geotechnics: Proceedings of the Third International Congress on Environmental Geotechnics Lisboa, Portugal. Balkema Rotterdam Brookfield, 7–11 September 1998, Vol. 2, pp. 449–454.

[3] D.G. Grubb, N. Sitar, Mobilization of trichloroethene (TCE) during ethanol flooding in uniform and layered sandpacks, Water Resour. Res. 35 (11) (1999) 3275.

[4] D.G. Grubb, N. Sitar, Horizontal ethanol floods in clean, uniform and layered sandpacks, Water Resour. Res. 35 (11) (1999) 3291.

[5] R.W. Falta, C.M. Lee, S.E. Brame, E. Roeder, J.T. Coates, C. Wright, A.L. Wood, C.G. Enfeld, Field test of high molecular weight alcohol flushing for subsurface nonaqueous phase liquid remediation, Water Resour. Res. 35 (7) (1999) 2095.

[6] P.S.C. Rao, M.D. Annable, R.K. Sillan, D. Dai, K. Hatfield, W.D. Graham, A.L. Wood, C.G. Enfield, Field-scale evaluation of in situ cosolvent flushing for enhanced aquifer remediation, Water Resour. Res. 33 (12) (1997) 2673.

[7] R.K. Sillan, M.D. Annable, P.S.C. Rao, D. Dai, K. Hatfield, W.D. Graham, A.L. Wood, C.G. Enfield, Evaluation of in situ cosolvent flushing dynamics using a network of spatially distributed multilevel samplers, Water Resour. Res. 34 (9) (1998) 2191.

[8] F. Schwille, Dense Chlorinated Solvents in Fractured and Porous Media: Model Experiments, in: J.F. Pankow (Ed.), Lewis Publishers, Chelsea, MI, 1988, 146 pp.

[9] USEPA, Basics of Pump-and-Treat Ground-Water Remediation Technology, EPA/600/8-90/003, Ada, OK, March 1990.

[10] K. Verschueren, Handbook of Environmental Data on Organic Chemicals, second ed., Van Nostrand Reinhold Company, New York, 1983, 1310 pp.

[11] CRC Handbook of Chemistry and Physics, in: D.R. Lide (Ed.), 76th ed., CRC Press, Boca Raton, 1995.

[12] R.J. Hunter, Introduction to Modern Colloid Science, Oxford University Press, New York, 1993, 344 pp.

[13] N. Sitar, J.R. Hunt, K.S. Udell, in: R.D. Woods (Ed.), Geotechnical Practice for Waste Disposal'87, Proceedings of a Specialty Conference sponsored by the Geotechnical Engineering Division of the American Society of Engineers, Ann Arbor, Michigan, ASCE, New York, 1987, pp. 205–223.

[14] D.G. Grubb, N. Sitar, Evaluation of Technologies for In-Situ Cleanup of DNAPL Contaminated Sites, EPA/600/R-94/120, Ada, OK, August 1994.